Variable stiffness composite patch for single-sided bonded repair of composite structures

Yashiro, Shigeki
Department of Aeronautics and Astronautics, Kyushu University

Akada, Ayari
Department of Aeronautics and Astronautics, Kyushu University

Onodera, Sota
Department of Aeronautics and Astronautics, Kyushu University

https://hdl.handle.net/2324/7358023

出版情報：Advanced Composite Materials. 34 (3), pp.495-512, 2024-11-10. Taylor and Francis
バージョン：

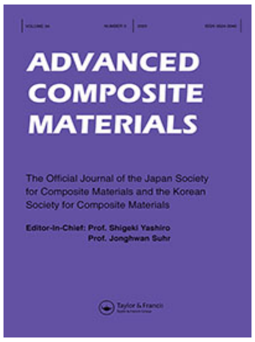

Taylor & Francis
Taylor & Francis Group

Advanced Composite Materials

ISSN: 0924-3046 (Print) 1568-5519 (Online) Journal homepage: www.tandfonline.com/journals/tacm20

Variable stiffness composite patch for single-sided bonded repair of composite structures

Shigeki Yashiro, Ayari Akada & Sota Onodera

To cite this article: Shigeki Yashiro, Ayari Akada & Sota Onodera (2025) Variable stiffness composite patch for single-sided bonded repair of composite structures, Advanced Composite Materials, 34:3, 495-512, DOI: 10.1080/09243046.2024.2425878

To link to this article: https://doi.org/10.1080/09243046.2024.2425878

Advanced Composite Materials, 2025
Vol. 34, No. 3, 495–512, https://doi.org/10.1080/09243046.2024.2425878

Variable stiffness composite patch for single-sided bonded repair of composite structures

Shigeki Yashiro, Ayari Akada and Sota Onodera

Department of Aeronautics and Astronautics, Kyushu University, 744 Motooka, Fukuoka, 819-0395, Japan

(*Received 18 August 2024; accepted 29 October 2024*)

Among several composite repair methods, single-sided bonded patch repair is a simple and time-effective method, but its post-repair tensile strength is usually low compared to that of double-sided repair and scarf repair. Despite the tensile loading, out-of-plane bending deformation is inevitable owing to the step-like load path and generates peel stress in the adhesive layer. This study proposes a variable stiffness (VS) patch that mitigates steep stiffness changes at the edge of the patch using a curvilinear fiber orientation and verifies its effectiveness in delaying patch debonding. The damage progress in the single-sided repaired quasi-isotropic CFRP laminate under tensile loading was predicted using three-dimensional finite element analysis with cohesive elements. Although patches debonded from one end in the loading direction, the VS patch with low stiffness near the end obtained a smaller out-of-plane deformation and a higher debonding onset strain than those of the standard quasi-isotropic patch. Furthermore, tensile tests of patch-repaired CFRP specimens demonstrated an increase in the debonding onset strain by the VS patch with a small variation. These results confirmed the effectiveness of the VS patch in the single-sided bonded repair of composite structures.

Keywords: polymer-matrix composite (PMCs); composite patch; single-sided repair; variable stiffness panel; debonding

1. Introduction

In recent years, carbon-fiber-reinforced plastics (CFRPs) have been increasingly used in the primary structures of airplanes and wind turbines owing to their high specific strength and modulus, and good fatigue properties. These composite structures can be damaged during operation, and their repair [1–3] should have high reliability and high work efficiency to shorten the maintenance period.

Scarf repair has been developed for composite structures; after removing the damaged area in a circular shape and machining its edge at a predetermined taper angle, the adhesive and prepreg are laminated and cured to fill the removal [4–8]. It has a high post-repair strength and small incremental aerodynamic drag in aircraft and wind turbines owing to its small surface irregularities. However, it usually takes a long time for careful machining operations and is thus unsuitable

Corresponding author. Shigeki Yashiro Email: yashiro@aero.kyushu-u.ac.jp

for temporary repairs. Bolted repair has been used in metal structures. After removing the damaged area, a prepared patch is bolted to cover the removal [4,5]. It requires less processing time and is suitable for temporary repairs; however, additional thickness, i.e. weight, is inevitable for composite structures to bear the stress concentration near the bolted holes. This study focuses on bonded repair, which uses adhesives to secure a patch to the damaged and removed area [4,5,9,10]. This method is as simple as bolted repair and does not suffer from stress concentrations. However, its post-repair strength is lower than that of the scarf repair. Improving the strength and reliability of bonded repair will lead to a high maintenance efficiency of the airframe.

The mechanical properties of bonded repairs have been characterized both experimentally and analytically in the literature. External patch bonding repair can be classified into two types: single-sided and double-sided. Double-sided repair is more effective than single-sided repair in terms of the stress intensity factor of the damage in the base plate [11], and many studies have been conducted on repair/joining using both sides of the base plate [9,12–18]. However, the back surface is not always accessible in real structures, in which case strength recovery is required by single-sided repair. In previous studies of single-sided repair, the strength and durability have been investigated with respect to the geometry (i.e. size, thickness, and shape) of the patch. Hou et al. [19,20] studied the low-velocity impact response of a CFRP cross-ply laminate with single-sided repair and investigated the relationship between the impact position and the delaminated area in the base plate. The optimal size, shape, and stacking sequence of the patch were also discussed analytically. Hall et al. [21] experimentally investigated low-velocity impact damage in single-sided patch repaired CFRP panels. Ultrasonic C-scan observations revealed that delamination was contained within the patch and that the surrounding base plate was not damaged by impact loading. Rachid et al. [22] analytically discussed the influence of the in-plane geometry of the boron/epoxy patch on the stress intensity factor of the crack in the base aluminum plate under tensile loading. Instead of the standard in-plane geometries, ‘H’ or arrow-shaped patches, which have a large bond area away from the repair site, improved the repair efficiency compared with a rectangular patch. Kashfuddoja et al. [23] investigated the displacement and strain fields of the adhesive layer in the single-sided patch repaired unidirectional CFRP specimen using the digital image correlation and finite element analysis. Load transfer from the base plate to the patch, i.e. the shear-lag mechanism, was observed near the longitudinal end of the patch. Their results suggested that the tapered patch end had a slight influence on strain reduction near the edge of the adhesive. Matta et al. [24] experimentally and numerically investigated the in-plane compression behavior of the open-hole CFRP plate with single-sided and double-sided bonded patches. The failure process started with the partial debonding of the patch(es). The patch debonding extended from the longitudinal end in the single-sided repair, whereas from both the longitudinal end and hole edge in the double-sided repair. The repaired specimens failed after complete separation of the patch(es).

In the case of single-sided repairs, a tensile load causes the patch to separate, and the repaired plate fails simultaneously. The reason for the premature failure of single-sided repair is the out-of-plane deformation called secondary bending [25–27]. When the patch is adhered to a single side, the neutral axis of bending changes in a step-like manner, as shown in Figure 1(a). Tensile loading then induces bending deformation, such that the neutral axis (i.e. the load path) becomes flat (Figure 1(b)). Such out-of-plane bending deformation is inevitable for single-sided repair. Both the shear and peel stresses are

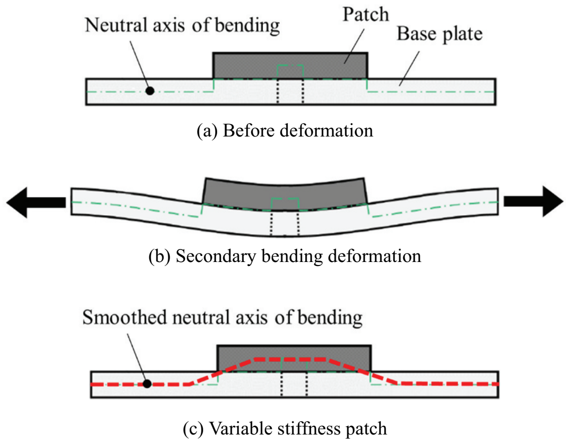

Figure 1. Schematic diagram of secondary bending and smoothing the neutral axis of bending.

severe at the edge of the adhesive layer, and the patches frequently separate before the final failure.

To address this difficulty, we focus on the method of changing the stiffness rather than the shape or size of the patch, and propose a variable stiffness (VS) patch. Moderating the step-like change in the neutral axis of bending, as shown in Figure 1(c), reduces secondary bending and delays the onset of debonding. The VS patch concept is more rigid at the center and less rigid at both ends. Automated fiber placement [28,29] and additive manufacturing [30,31] can continuously steer the fiber direction, and variable-stiffness panels using curvilinear fiber placement have been studied in recent years [32–35]. Therefore, patches with continuously varying stiffness can be realized by designing the fiber orientation within a ply.

Thus, the purpose of this study is to demonstrate the effectiveness of VS patches in improving the reliability of single-sided patch repair. To this end, a finite element analysis and tensile tests of single-sided patch-repaired CFRP plates are conducted. The remainder of this paper is organized as follows. In Section 2, a finite element analysis of the patch debonding progress is described, and the effect of the VS patch on debonding onset is investigated. In Section 3, tensile tests using the quasi-isotropic (QI) patch and VS patch are conducted, and the advantages of the VS patch are discussed. Finally, the conclusions of this study are presented in Section 4.

2. Analysis

2.1. *Analytical model*

The debonding process of the patch from the base CFRP laminate plate was predicted to verify the concept of a VS patch for single-sided repair. The commercial finite element analysis software ABAQUS 2019. HF6 was used in this study. Figure 2 shows the finite element model, which consists of a CFRP base plate, CFRP patch, and film adhesive. The base plate with the QI stacking sequence $[45/0/-45/90]_S$ has an open hole at the center as the removal of a damaged part. The base plate was 190 mm long, 39 mm wide, and 1 mm thick, and the hole diameter was 10 mm. Four patches were examined in this study: one had the same QI stacking sequence as the base plate, and the others had

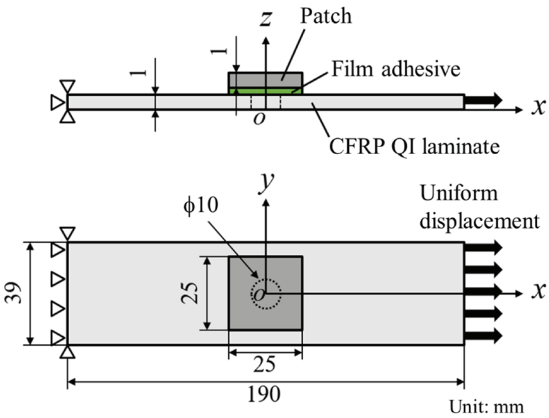

(a) Dimensions

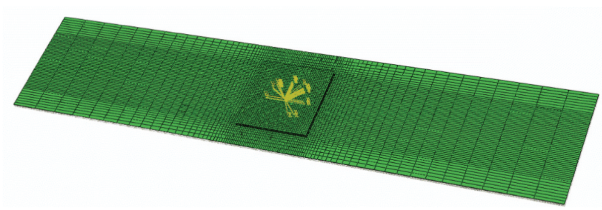

(b) Finite element mesh

Figure 2. Analytical model of a patch repaired composite plate.

curvilinear fiber orientations (described in detail in the following section). The patch was 25 mm square and 1 mm thick; the geometry of the patch against the base plate was based on Ref. [36], where the QI patch did not show sufficient repair efficiency. The base plate and patch were divided into eight plies, each of which was transversely isotropic. The film adhesive 0.2 mm thick had isotropic material properties. The material properties are listed in Table 1. Eight-node hexahedral solid elements were used, with 52,524 solid elements and 116,282 nodes. It is noted that increasing the number of divisions in the through-thickness direction or using the second-order solid elements is required for more

Table 1. Material properties used in the analysis [37,38].

(a) CFRP	
Longitudinal Young's modulus (GPa)	135
Transverse Young's modulus (GPa)	8.2
In-plane Poisson's ratio	0.31
Out-of-plane Poisson's ratio	0.4
In-plane shear modulus (GPa)	4.8
Out-of-plane shear modulus (GPa)	3.5
(b) Film adhesive	
Young's modulus (GPa)	3.0
Poisson's ratio	0.42

accurate analysis. The longitudinal end of the model was fixed, and a uniform tensile displacement was applied to the other end.

Crack growth at the interface between the patch and the adhesive layer was assumed, and Abaqus built-in eight-node cohesive elements were inserted into the interface. A bi-linear relationship between the traction and relative displacement was assumed, and parameters typical for the interface between the CFRP and adhesive were used for the strength (50 MPa) and fracture toughness (2 kJ/m^2) to identify differences in the debonding process owing to the patch configurations. The quadratic stress criterion was used to initiate damage, and damage evolution was considered when the mixed-mode energy release rate reached the fracture toughness.

2.2. *Analysis cases*

When a standard patch with uniform stiffness is adhered to a single side, the load path is stair-stepped in the through-thickness direction. Tensile loading then causes secondary bending, such that the load path approaches a straight line, and out-of-plane deformation generates a severe stress state in the adhesive layer. Therefore, the VS patch requires low stiffness near the end to mitigate the steep changes in the load path. A local stiffness change can be realized by steering the carbon fibers. The fiber orientation in the VS patch investigated in this study is illustrated in Figure 3. The patch size was 25 mm square. The fundamental stacking sequence is quasi-isotropic $[45/0/-45/90]_S$, and in the 5-mm region at both ends, the fiber orientation was changed to 60° for the 45° ply, 45° for the 0° ply, and −60° for the −45° ply. Furthermore, a double-steered VS patch with

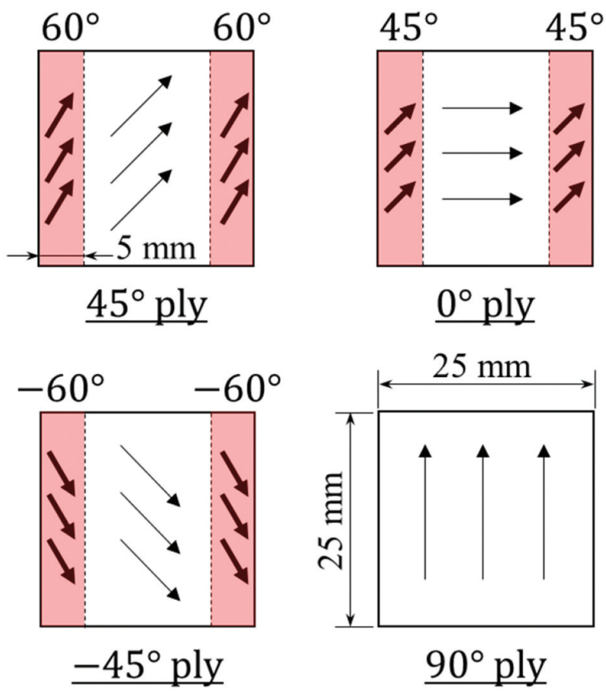

Figure 3. Lamination structure of the VS patch. Fiber orientation in the end regions is steered to reduce the stiffness.

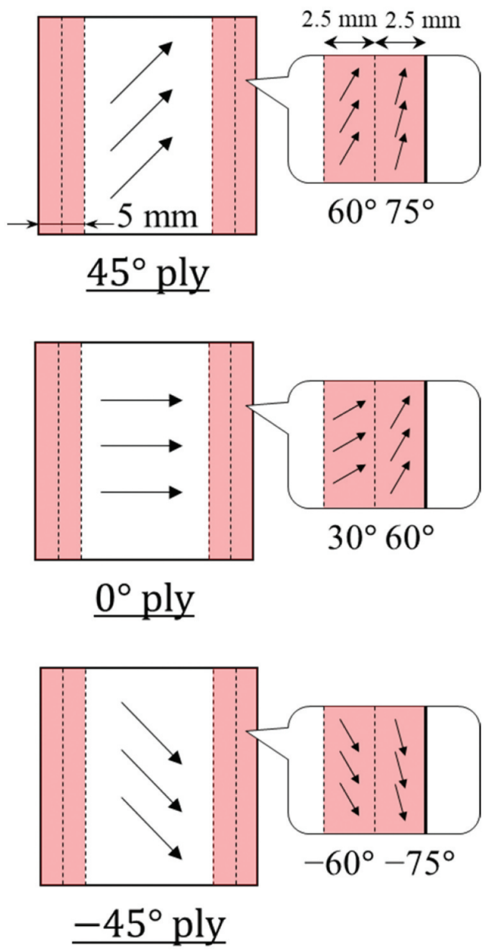

Figure 4. Lamination structure of the double-steered patch.

a smaller stiffness change was also considered by dividing the end region into two parts (Figure 4).

The following four analyses were conducted. The reference analysis used a standard QI patch with uniform stiffness (case #1). The effectiveness of stiffness control was investigated using a single-steered VS patch (case #2) and a double-steered VS patch (case #3). Moreover, the influence of the width of the fiber steering region on the debonding process was investigated by increasing the width (10 mm) with the fiber orientation shown in Figure 3 (case #4).

2.3. *Analysis results*

The predicted stress–strain curves are shown in Figure 5. The stress is the sum of the nodal forces on the longitudinal end surface divided by the cross-sectional area far from the patch, and the strain is the applied displacement divided by the length of the base plate. In case #1 with the QI patch, as shown in the traction distribution in Figure 6, the

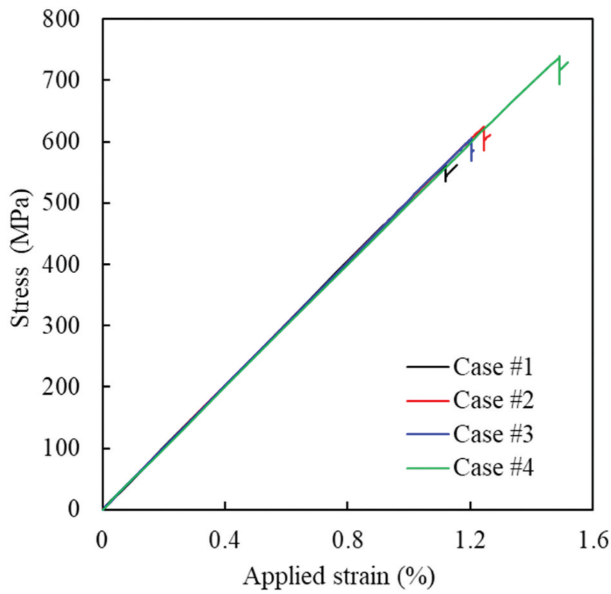

Figure 5. Predicted stress–strain curves in tensile analysis of patch repaired CFRP plates.

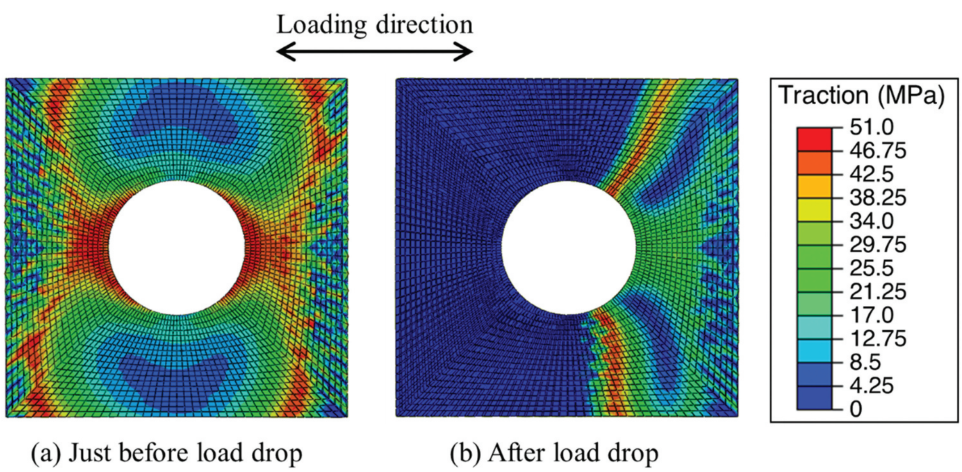

Figure 6. Effective traction distribution at 1.12% applied strain in analysis case #1.

patch debonded unstably at 1.12% applied strain, and the stress decreased abruptly. Figure 7(a) (black) shows the out-of-plane displacement of the width-wise centerline of the patch just before the QI patch debonded. The patch was convexly deformed downward, indicating secondary bending.

In cases #2 and #3, similar to the QI patch, the VS patches debonded rapidly and the stress decreased abruptly as shown in Figure 5, but the applied strain of debonding (1.25% and 1.2%, respectively) was higher than that of the QI patch. The out-of-plane deformations of cases #2 and #3 are shown in Figure 7(a). The displacement at the end of the VS patches was smaller than that of the QI patch at an applied strain of 1.12%, at

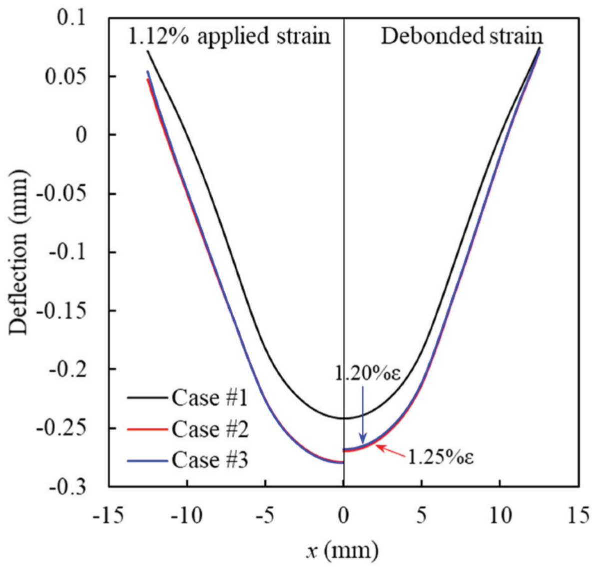

(a) Comparison by fiber steering patterns

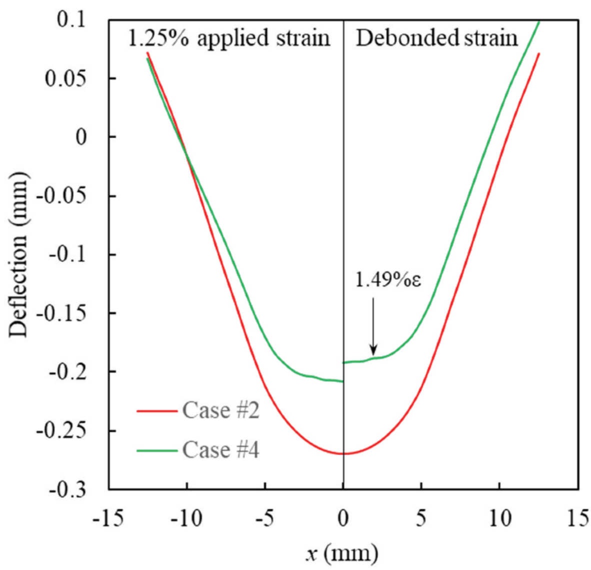

(b) Comparison by fiber steering widths

Figure 7. Out-of-plane displacement at the center of the patch in the transverse direction. The displacement distribution is symmetric about $x = 0$. The left half shows the distribution at the strain just before debonding in the reference case, and the right half shows the distribution at the strain just before debonding in each case.

which point the QI patch debonded. Therefore, the effect of the VS patch on the relaxation of secondary bending was analytically demonstrated. Comparing cases #2 and #3, there was no positive effect on patch debonding by two-step fiber steering in the patch end region.

In case #4, where the width of the fiber steering region was 10 mm, patch debonding developed rapidly as in cases #1 and #2, but the applied strain of separation was 1.49%, which was significantly higher than that in case #2. Figure 7(b) compares the out-of-plane deformation of the patch in case #4 with that in case #2. The displacement at the end of the patch in case #4 was the same as that in case #2 at 1.25% applied strain. However, the deflection at the center of the patch in case #4 was smaller than that in case #2, and patch debonding was further delayed by reducing secondary bending. Therefore, it is suggested that the size of the fiber steering (i.e. low stiffness) region of the patch has a significant effect on the post-repair strength.

3. Experiment

3.1. *Materials and setup*

The effect of the VS patch on delaying patch debonding was experimentally verified. The dimensions of the patch-repaired CFRP coupon specimen were the same as those of the analysis model (Figure 2): the base plate was 240 mm long, 39 mm wide, and 1 mm thick, with an open hole of 10 mm diameter, and the patch was 25 mm square and 1 mm thick. GFRP end tabs, 25 mm long and 1 mm thick, were attached to alleviate stress concentration by gripping. The thickness of the adhesive layer was 0.2 mm. The stacking sequence of the base plate was $[45/0/-45/90]_S$. A uniform stiffness QI $[45/0/-45/90]_S$ patch and a single-steered VS patch were prepared. To steer the fiber orientation in the VS patch, a prepreg sheet was warmed gently using an electric hot plate (70°C), and the fibers near both ends were oriented to the angle prescribed in Figure 3 using glass sheets [39], as depicted in Figure 8. The materials used were standard multi-purpose CFRP prepreg T700SC/#2500 (Toray Industries) and film adhesive FM300K (Cytec) used for composite-to-composite and composite-to-metal bonding. The stacked prepreg sheets

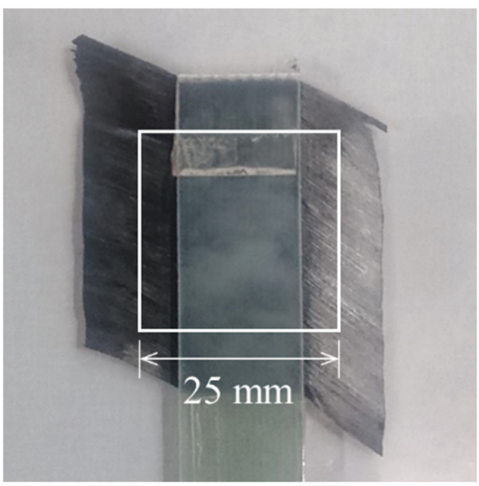

Figure 8. Image of the 0° ply in the VS patch with the fiber orientation modified at the ends.

were cured using a vacuum hot-press process at 135°C temperature for 2 h. After fabricating the base plate and patch separately, the bonding area was sanded and cleaned, and the patch was then adhered to the base plate using the film adhesive at 175°C temperature for 1 h.

Quasi-static tensile tests of the patch-repaired CFRP specimens were conducted at a crosshead speed of 0.3 mm/min using a universal testing machine (AG-50kNXDplus, Shimadzu). The load, crosshead displacement, and strain were simultaneously measured. Because tensile loading causes secondary bending deformation, strain gauges were attached to both sides of the base plate away from the patch and at the center of the patch.

3.2. *Results and discussion*

Figure 9(a) presents the stress–strain curves obtained using the QI patch. The stress is the load divided by the cross-sectional area of the flat part; the solid line is the average of the two strains on both sides of the base plate away from the patch, and the dashed line is the strain at the center of the patch. Although the former strain increased linearly with increasing applied stress, the latter strain changed nonlinearly owing to secondary bending. The strain on the patch then decreased at an almost constant stress. The adhesion area, when the strain on the patch was reduced, was observed using additional specimens via a soft X-ray radiography system (M100, Softex). Contrast agent was applied to the patch periphery. The soft X-ray image in Figure 10(a) shows that the patch debonded from an end at an applied stress of 460–520 MPa and rapidly lost its load-bearing capacity, resulting in a decrease in the strain on the patch. Because the base plate did not break even after one-half of the patch was completely separated, the applied stress increased, while the strain on the patch remained at approximately 0.1% until final failure. Figure 9(b) shows the stress–strain curves when using the VS patch. As with the QI patch, the VS patch lost its load-bearing capacity before the final failure owing to debonding, and the strain on the patch decreased despite the increase in the applied stress. Half of the VS patch was separated at an applied stress of approximately 500 MPa as shown in Figure 10(b).

The average strength of the specimens with QI patches was 554 MPa and that of the specimens with VS patches was 544 MPa, showing no significant difference between them. This was because the patches lost their load-bearing capacity before the final failure. Therefore, strength is not appropriate for evaluating the effectiveness of the patch. Instead, the applied strain when the maximum strain was reached on the patch is defined as the debonding onset strain, as shown in Figure 11. Table 2 summarizes the debonding onset strain and the applied stress at that moment. The debonding onset strain of the VS patch (0.96%) was higher than that of the QI patch (0.90%) and its variability was smaller than that of the QI patch. The stress applied when the debonding onset strain was reached using the VS patch was approximately 30 MPa higher than that when using the QI patch. Thus, the effect of the VS patch on delaying the debonding onset was experimentally confirmed.

Figure 12 presents an overview of the specimens after failure. No significant difference between the two patches was observed on the separated surface, and cohesive failure occurred with the adhesive remaining on both the patch and the base plate.

To prevent premature failure and to increase the efficiency of strength recovery, tensile tests were performed on coupon specimens with 35-mm-long patches. Specimens

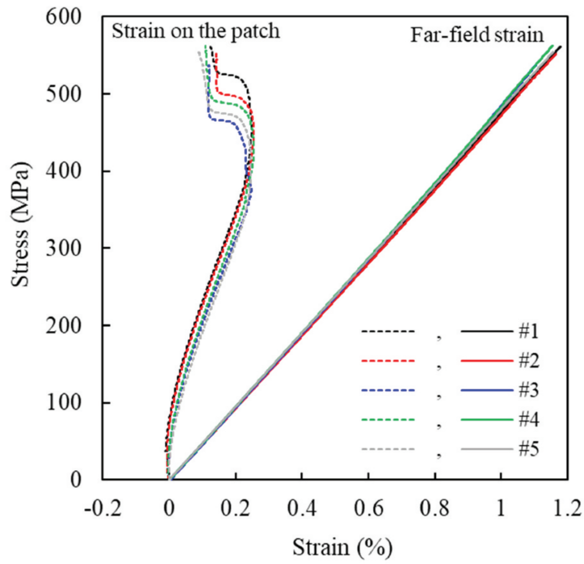

(a) QI patch

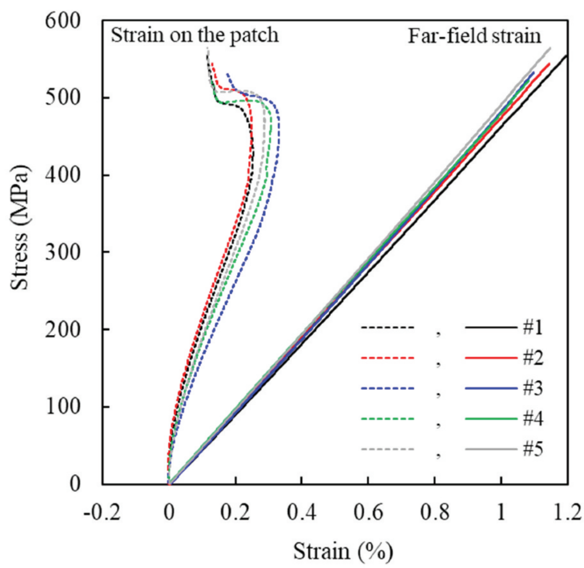

(b) VS patch

Figure 9. Stress–strain curves in the tensile tests of patch repaired CFRP plates.

with QI and VS patches were tested, and the fibers were steered within a 5 mm area at both ends in the VS patch. Figure 13 presents the measured stress–strain curves. The average strength was 589 MPa for the QI patch and 583 MPa for the VS patch, which was greater than that obtained using a patch 25 mm long. There was no significant difference in average strength between the QI and VS patches. However, for the QI patches, two patterns appeared: one-half of the patch separated before the final failure in

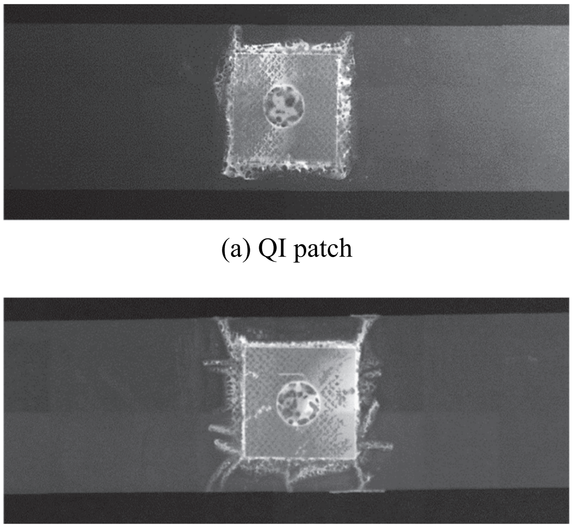

(a) QI patch

(b) VS patch

Figure 10. Soft X-ray photograph of the specimen after the strain on the patch decreased.

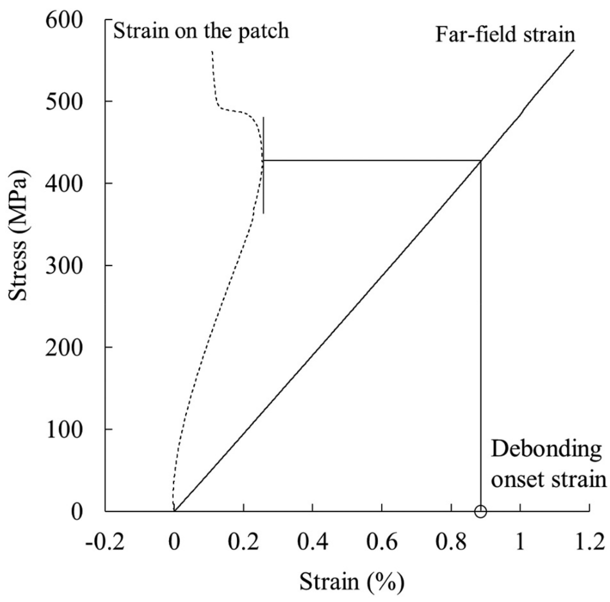

Figure 11. Schematic illustration of the debonding onset strain.

specimen #1, and failure occurred during the rapid progress of patch debonding in #2 and #3. Different failure patterns resulted in a wide variety of strengths. In contrast, all specimens using the VS patch failed during the debonding process. The debonding onset strain of the VS patch was higher and less varied than that of the QI patch (Table 3). The

Table 2. Summary of the test results using the patches 25 mm long.

	Strain on the patch (%)	Debonding onset strain (%)	Applied stress (MPa)
(a) QI patch			
#1	0.248	0.975	463.7
#2	0.254	0.962	453.8
#3	0.247	0.788	376.1
#4	0.254	0.879	423.9
#5	0.244	0.889	425.3
Average		0.899	428.6
Standard deviation		0.067	30.5
(b) VS patch			
#1	0.253	0.933	430.8
#2	0.249	0.980	464.9
#3	0.332	0.956	459.6
#4	0.308	0.966	463.5
#5	0.288	0.961	471.0
Average		0.959	457.9
Standard deviation		0.015	14.1

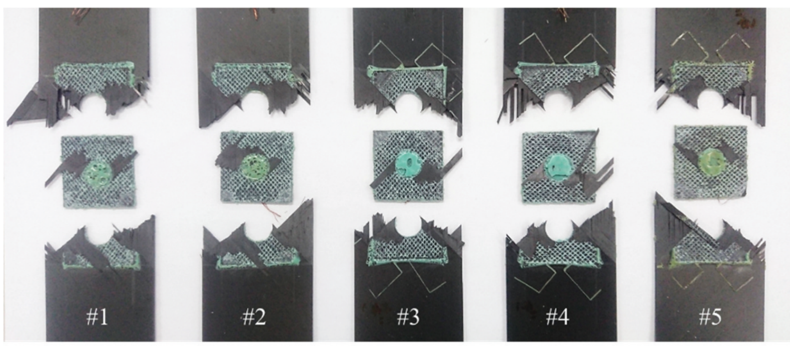

(a) QI patch

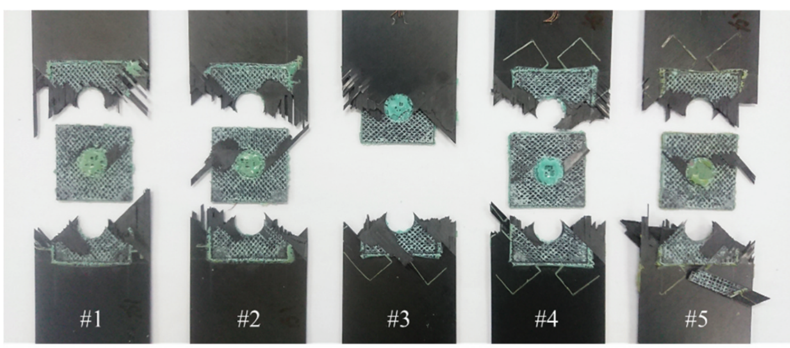

(b) VS patch

Figure 12. Overview of the failed specimens.

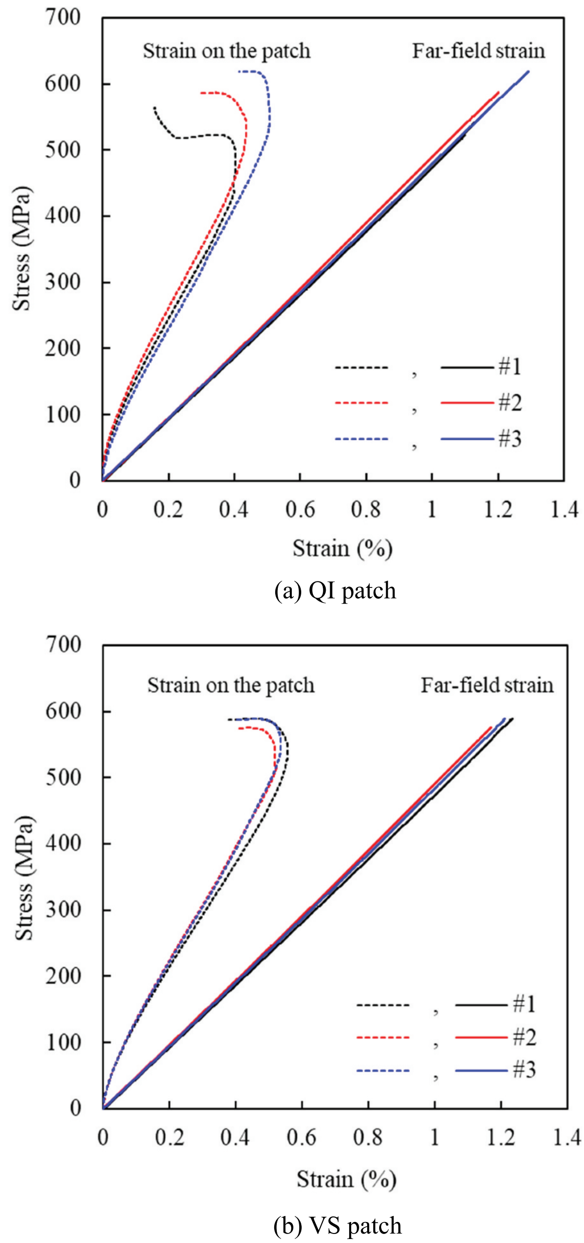

Figure 13. Stress–strain curves in the tensile test of CFRP plate repaired with long patch.

small variation in the debonding onset strain and strength by the VS patch suggests that the low-stiffness region reduces the impact of the adhesion quality on patch debonding.

These experimental results demonstrate the advantage of the VS patch in delaying debonding. However, the improvement in debonding onset strain by the VS patch was reduced when the patch was elongated. If the size of the fiber steering area and its stacking configuration (i.e. stiffness) are optimized according to the overall dimensions,

Table 3. Summary of the test results using the patches 35 mm long.

	Strain on the patch (%)	Debonding onset strain (%)	Applied stress (MPa)
(a) QI patch			
#1	0.404	1.023	484.8
#2	0.436	1.097	537.7
#3	0.507	1.147	550.1
Average		1.089	524.2
Standard deviation		0.051	28.3
(b) VS patch			
#1	0.557	1.136	540.0
#2	0.524	1.054	517.7
#3	0.536	1.132	549.1
Average		1.107	535.6
Standard deviation		0.038	13.2

the use of the VS patch will further improve the debonding resistance and post-repair strength compared to conventional single-sided patch repairs.

In summary, compared with the use of the QI patch, the VS patch reduces the out-of-plane displacement and cohesive traction near the longitudinal edge of the patch, where patch debonding is initiated. In practical situations, such as aircraft structural components, a patch-repaired component experiences cyclic and creep loading under varying environmental conditions. Reducing traction in the adhesive layer delays stress-induced plasticization and the formation of microscopic damage, and improves long-term durability. However, it is noted that the effectiveness of patch repair is inferior to that of scarf repair, unless the patch is considerably larger than the area of damage removal, allowing for an increase in weight. Even with a VS patch, secondary bending is unavoidable as long as the patch is repaired from one side. The repair efficiency (i.e. the ratio of the post-repair strength to the pristine laminate strength) was approximately 60% for the 35-mm-long patch in this study. In contrast, the repair efficiency using scarf repair was 64–80% depending on the repair design [40].

In this study, the VS patches were characterized in a simple uniaxial tensile loading situation, which is a limitation of this study. In practical cases, the structural components are subjected to biaxial and complex loading. In such cases, fiber steering only at the opposite ends, as shown in Figure 3, may not be sufficient. For more complex cases, detailed studies, including the optimization of the range of fiber steering and fiber orientation angles, are required.

4. Conclusions

In this study, a VS patch was proposed for single-sided repair, and its effectiveness was verified both analytically and experimentally. Finite element analysis was performed to predict the debonding process of the patch and identify the advantage of the VS patch over the standard patch with uniform stiffness. Quasi-static tensile tests were also conducted on CFRP laminates with single-sided repair. The conclusions of this study are summarized below.

(1) The finite element analysis demonstrated that the VS patch with reduced stiffness near the longitudinal ends relaxed the secondary bending and delayed debonding compared to the QI patch with uniform stiffness. In addition, the larger the fiber steering region, the greater is the applied strain at which debonding occurred.
(2) In the tensile tests of the patch-repaired CFRP plate, the patch 25 mm long debonded from one end to the hole and lost the load-bearing capacity before final failure, regardless of the type of patch. However, the debonding onset strain of the VS patch was higher than that of the QI patch. Reducing the stiffness near the patch ends delayed debonding.
(3) Specimens repaired with the patch 35 mm long broke by rapid debonding of the patch regardless of the type of patch, showing a strength recovery effect of patch repair. Again, the debonding onset strain of the VS patch was higher and less varied than that of the QI patch.

These experiments and analyses demonstrated the effect of the VS patch on delaying debonding onset by mitigating secondary bending. VS patches have several degrees of freedom, including the overall size, size of the fiber steering region, and stiffness distribution. The optimization of these parameters for each structural application, including multiaxial loading, is the subject of our future study.

Disclosure statement

No potential conflict of interest was reported by the author(s).

Funding

A part of this work was supported by JSPS KAKENHI Grant Number [23K26299].

ORCID

Shigeki Yashiro http://orcid.org/0000-0001-5266-2039

References

[1] Zhou W, Ji X, Yang S, et al. Review on the performance improvements and non-destructive testing of patches repaired composites. Compos Struct. 2021;263:113659. doi: 10.1016/j.compstruct.2021.113659
[2] Kim M, Kim H, Lee W. Repair of aircraft structures using composite patches bonded through induction heating. Adv Compos Mater. 2015;24(4):307–323. doi: 10.1080/09243046.2014.899553
[3] Bao L, Maruyama Y, Shi J. Mechanisms of solid particle erosion damage in the repair of damaged composite structures. Adv Compos Mater. 2022;31(4):385–398. doi: 10.1080/09243046.2021.2018090
[4] Niu M-Y. Composite airframe structures: practical design information and data. Wanchai, Hong Kong: Conmilit Press; 1993.
[5] Katnam KB, Da Silva LFM, Young TM. Bonded repair of composite aircraft structures: a review of scientific challenges and opportunities. Prog Aerosp Sci. 2013;61:26–42. doi: 10.1016/j.paerosci.2013.03.003
[6] Wang CH, Gunnion AJ. Optimum shapes of scarf repairs. Compos Part A. 2009;40(9):1407–1418. doi: 10.1016/j.compositesa.2009.02.009

[7] Breitzman TD, Iarve EV, Cook BM, et al. Optimization of a composite scarf repair patch under tensile loading. Compos Part A. 2009;40(12):1921–1930. doi: 10.1016/j.compositesa.2009.04.033
[8] Truong V-H, Yoo J-S, Kim C-H, et al. Failure load prediction of laminates repaired with a scarf-bonded patch using the damage zone method. Adv Compos Mater. 2016;26(2):115–133. doi: 10.1080/09243046.2016.1232008
[9] Cheng P, Gong X-J, Hearn D, et al. Tensile behaviour of patch-repaired CFRP laminates. Compos Struct. 2011;93(2):582–589. doi: 10.1016/j.compstruct.2010.08.021
[10] Mohammadi S, Yousefi M, Khazaei M. A review on composite patch repairs and the most important parameters affecting its efficiency and durability. J Reinf Plast Compos. 2021;40(1–2):3–15. doi: 10.1177/0731684420941602
[11] Albedah A, Bachir Bouiadjra B, Mhamdia R, et al. Comparison between double and single sided bonded composite repair with circular shape. Mater Des. 2011;32(2):996–1000. doi: 10.1016/j.matdes.2010.08.022
[12] Campilho RDSG, de Moura MFSF, Ramantani DA, et al. Tensile behaviour of three-dimensional carbon-epoxy adhesively bonded single- and double-strap repairs. Int J Adhes Adhes. 2009;29(6):678–686. doi: 10.1016/j.ijadhadh.2009.02.004
[13] Liu X, Wang G. Progressive failure analysis of bonded composite repairs. Compos Struct. 2007;81(3):331–340. doi: 10.1016/j.compstruct.2006.08.024
[14] Cheng P, Gong X-J, Aivazzadeh S, et al. Experimental observation of tensile behavior of patch repaired composites. Polym Test. 2014;34:146–154. doi: 10.1016/j.polymertesting.2014.01.007
[15] Bhatia GS, Andrew JJ, Balaganesan G, et al. The role of patch-parent configurations on the tensile response of patch repaired carbon/epoxy laminates. Polym Test. 2018;70:413–425. doi: 10.1016/j.polymertesting.2018.07.025
[16] Yashiro S, Wada J, Sakaida Y. A monitoring technique for disbond area in carbon fiber–reinforced polymer bonded joints using embedded fiber bragg grating sensors: development and experimental validation. Struct Health Monit. 2017;16(2):185–201. doi: 10.1177/1475921716669979
[17] Oshima S, Yoshimura A, Yashiro S, et al. Experimental and analytical validation of mode II fracture toughness tests for a type of double-lap joint. Compos Struct. 2020;234:111757. doi: 10.1016/j.compstruct.2019.111757
[18] Kumabe S, Yashiro S, Onodera S. Evaluation of the frictional effect on the energy release rate in doubly end-notched tension test for mode II delamination. Eng Fract Mech. 2023;288:109354. doi: 10.1016/j.engfracmech.2023.109354
[19] Tie Y, Hou Y, Li C, et al. An insight into the low-velocity impact behavior of patch-repaired CFRP laminates using numerical and experimental approaches. Compos Struct. 2018;190:179–188. doi: 10.1016/j.compstruct.2018.01.075
[20] Hou Y, Tie Y, Li C, et al. Low-velocity impact behaviors of repaired CFRP laminates: effect of impact location and external patch configurations. Compos Part B. 2019;163:669–680. doi: 10.1016/j.compositesb.2018.12.153
[21] Hall ZEC, Liu J, Brooks RA, et al. The effectiveness of patch repairs to restore the impact properties of carbon-fibre reinforced-plastic composites. Eng Fract Mech. 2022;270:108570. doi: 10.1016/j.engfracmech.2022.108570
[22] Rachid M, Serier B, Bouiadjra BB, et al. Numerical analysis of the patch shape effects on the performances of bonded composite repair in aircraft structures. Compos Part B. 2012;43(2):391–397. doi: 10.1016/j.compositesb.2011.08.047
[23] Kashfuddoja M, Ramji M. Assessment of local strain field in adhesive layer of an unsymmetrically repaired CFRP panel using digital image correlation. Int J Adhes Adhes. 2015;57:57–69. doi: 10.1016/j.ijadhadh.2014.10.005
[24] Matta S, Kolanu NR, Chinthapenta V, et al. Progressive damage analysis of adhesively bonded patch repaired carbon fibre–reinforced polymer specimen under compression involving cohesive zone model. Int J Damage Mech. 2019;28(10):1457–1489. doi: 10.1177/1056789519832062
[25] Wang CH, Rose LRF. On the design of bonded patches for one-sided repair. In: Proceedings of ICCM-11; Gold Coast, Australia; 1997 July; Vol VI. p. 347–356.
[26] Wang CH, Rose LRF, Callinan R. Analysis of out-of-plane bending in one-sided bonded repair. Int J Solids Struct. 1998;35(14):1653–1675. doi: 10.1016/S0020-7683(97)00129-7

[27] Clark RJ, Romilly DP. Linear coupled bending and extension of an unbalanced bonded repair. Int J Solids Struct. 2007;44(10):3156–3176. doi: 10.1016/j.ijsolstr.2006.09.012
[28] Frketic J, Dickens T, Ramakrishnan S. Automated manufacturing and processing of fiber-reinforced polymer (FRP) composites: an additive review of contemporary and modern techniques for advanced materials manufacturing. Addit Manuf. 2017;14:69–86. doi: 10.1016/j.addma.2017.01.003
[29] Onodera S, Kawahara K, Yashiro S. Damage progression and strength prediction of open-hole CFRP laminates containing ply gaps. Eng Fract Mech. 2023;293:109681. doi: 10.1016/j.engfracmech.2023.109681
[30] van de Werken N, Tekinalp H, Khanbolouki P, et al. Additively manufactured carbon fiber-reinforced composites: state of the art and perspective. Addit Manuf. 2020;31:100962. doi: 10.1016/j.addma.2019.100962
[31] Kajimoto J, Fujii A, Maruyama Y, et al. Automatic strengthening in thickness direction using lap joint of carbon fiber for fused filament fabrication 3D printing. Compos Struct. 2023;303:116290. doi: 10.1016/j.compstruct.2022.116290
[32] Demir E, Yousefi-Louyeh P, Yildiz M. Design of variable stiffness composite structures using lamination parameters with fiber steering constraint. Compos Part B. 2019;165:733–746. doi: 10.1016/j.compositesb.2019.02.004
[33] Malakhov AV, Polilov AN, Zhang J, et al. A modeling method of continuous fiber paths for additive manufacturing (3D printing) of variable stiffness composite structures. Appl Compos Mater. 2020;27(3):185–208. doi: 10.1007/s10443-020-09804-8
[34] Lozano GG, Tiwari A, Turnet C, et al. A review on design for manufacture of variable stiffness composite laminates. Proc Inst Mech Eng Part B-J Eng Manuf. 2015;230(6):981–992. doi: 10.1177/0954405415600012
[35] Fayazbakhsh K, Nik MA, Pasini D, et al. Defect layer method to capture effect of gaps and overlaps in variable stiffness laminates made by automated fiber placement. Compos Struct. 2013;97:245–251. doi: 10.1016/j.compstruct.2012.10.031
[36] Yoshitake H, Wang W-X, Matsubara T. A study on the improvement of the recovery rate of CFRP laminate with a single patch adhesive repair. In: Annual Conference of the Japan Society for Aeronautical and Space Sciences Western Branch; Fukuoka; 2018 Nov 22; JSASS-2018-S038 (in Japanese).
[37] Yashiro S, Ogi K. Fracture behavior in CFRP cross-ply laminates with initially cut fibers. Compos Part A. 2009;40(6–7):938–947. doi: 10.1016/j.compositesa.2009.04.023
[38] Guedes RM, de Moura MFSF, Ferreira FJ. Failure analysis of quasi-isotropic CFRP laminates under high strain rate compression loading. Compos Struct. 2008;84(4):362–368. doi: 10.1016/j.compstruct.2007.10.001
[39] Yoshida T, Minakuchi S. Improving fatigue characteristics of ply drop-off in composite laminate with ply curving termination. Adv Compos Mater. articles in press. doi: 10.1080/09243046.2024.2329364
[40] Damghani M, Bolanos S, Chahar A, et al. Design, novel quality check and experimental test of an original variable length stepped scarf repair scheme. Compos Part B. 2022;230:109542. doi: 10.1016/j.compositesb.2021.109542